

miR-372-3p promotes preeclampsia progression by regulating twist1

ZIWEI LI^{1,2}, JIE WANG^{1,2}, DIANTING LI¹, HAIYING CHEN¹ and TAO MENG¹

¹Department of Obstetrics, The First Affiliated Hospital of China Medical University;

²Department of Obstetrics and Gynecology, China Medical University, Shenyang, Liaoning 110001, P.R. China

Received March 29, 2021; Accepted August 24, 2021

DOI: 10.3892/etm.2022.11659

Abstract. Preeclampsia (PE) is a common pregnancy-related disorder worldwide. PE is mainly characterized by the defective migration and invasion of trophoblast cells. MicroRNAs (miRs) have been reported to serve an important role in PE. The purpose of the study was to explore the pathogenesis and therapeutic targets of preeclampsia. In the present study, reverse transcription-quantitative PCR analysis revealed that the expression levels of miR-372-3p were upregulated in placental tissues from patients with PE. Notably, the expression levels of miR-372-3p were significantly upregulated in patients with early-onset PE compared with patients with late-onset PE. Moreover, *in vitro* analysis using wound healing, Transwell and western blotting assays demonstrated that miR-372-3p overexpression inhibited the migration, invasion and epithelial-mesenchymal transition (EMT) of HTR-8/SVneo trophoblast cells, respectively. Bioinformatics analysis and a dual luciferase reporter assay revealed that miR-372-3p is sponged by twist family bHLH transcription factor 1 (twist1). Rescue experiments found that miR-372-3p overexpression suppressed trophoblast cell migration, invasion and EMT by downregulating the expression of twist1. In conclusion, the present study revealed that high level of miR-372-3p may act as a factor to cause PE and may also be a potential novel therapeutic target for PE.

Introduction

Preeclampsia (PE) refers to new-onset hypertension after 20 weeks of pregnancy that is accompanied by proteinuria, headaches, vertigo, nausea, vomiting, epigastric discomfort (1). PE is a severe obstetric emergency worldwide, with

an annual incidence rate of 2-8%, and is the leading cause of increased morbidity and mortality rates in pregnant women and newborns (2). Therefore, understanding the mechanisms underlying the onset of PE remains an urgent priority for obstetricians. Insufficient invasion of extravillous trophoblasts (EVTs) was suggested to be the leading cause of PE, which results in reduced anchorage of EVT to the endometrium and decreased vascular remodeling. The insufficiently remodeled blood vessel clusters at the maternal-fetal interface and is unable to withstand the huge volume of blood in the later trimester, leading to high blood pressure and the vascular endothelial cells subsequently releasing various inflammatory factors, which induces the clinical symptoms of hypertension and eclampsia (3,4).

MicroRNAs (miRNAs/miRs) are non-coding RNAs that have been revealed to serve regulatory roles in various pathological or physiological processes (5-8), including placental development (9). Several miRNAs have been found to modulate trophoblast cells. For example, miR-145-5p facilitated PE development by affecting the proliferation and invasion of trophoblast cells (10); miR-218-5p was shown to promote trophoblast invasion and endovascular EVT differentiation by regulating the miR-218-5p/TGFβ2 signaling pathway (11); and the expression levels of miR-221-3p were found to be downregulated in PE and promoted trophoblast proliferation, invasion and migration, at least partly, by targeting thrombospondin 2 (12). However, how miRNAs affect trophoblast cell biological behaviors requires further investigations.

The present study revealed that miR-372-3p was associated with the occurrence of PE and that it suppressed trophoblast cell migration, invasion and epithelial-mesenchymal transition (EMT) by regulating twist1. These findings may provide a potential novel biomarker or therapeutic target for PE.

Materials and methods

Patient studies. A total of 59 pregnant (maternal age shown in Table I) women who had undergone a cesarean section at the Obstetrics Department of The First Hospital of China Medical University (Shenyang, China) were recruited for this study between October 2018 and October 2020. A diagnosis of PE with severe features defined using the following criteria: i) Systolic blood pressure ≥ 160 mmHg or diastolic blood pressure ≥ 110 mmHg; and ii) 24 h urine

Correspondence to: Professor Tao Meng, Department of Obstetrics, The First Affiliated Hospital of China Medical University, 155 North Nanjing Road, Shenyang, Liaoning 110001, P.R. China
E-mail: cmumtxzy@163.com

Key words: preeclampsia, trophoblast, microRNA-372-3p, epithelial-mesenchymal transition, twist family bHLH transcription factor 1

protein >300 mg and protein/creatinine ≥ 0.3 . In the case of negative urine protein, the following new manifestations are met: i) Thrombocytopenia, platelet count $< 100 \times 10^9/l$; ii) renal insufficiency, serum creatinine $> 97 \mu\text{mol/l}$ or 2 times higher compared with the upper limit of normal, excluding other kidney diseases; iii) impaired liver function, transaminase is 2 times higher compared with the upper limit of normal; iv) pulmonary edema; and v) new headache that common medication does not relieve one other causes or blurred vision have been ruled out according to the diagnostic criteria of The American College of Obstetricians and Gynecologists (1) was used as the inclusion criterium to avoid the influence of non-placental factors. The following exclusion criteria were used for recruitment: i) Twin pregnancy; and ii) diagnosis of gestational diabetes, renal disease, chronic hypertension, acute or chronic hepatitis, hyperthyroidism or hypothyroidism. Patients with hypertension, proteinuria, twin pregnancy, diagnosis of gestational diabetes, renal disease, chronic hypertension, acute or chronic hepatitis, hyperthyroidism and hypothyroidism were excluded. According to the gestational age, the 59 patients were divided into early-onset PE (EOPE; ≤ 34 weeks), late-onset PE (LOPE; > 34 weeks), pre-term delivery (ENP) and full-term delivery (NP tissues) groups. Control groups were set according to gestational age. The method of placenta collection in the NP group was the same as that in the PE group. Patients in the NP group were recruited to try to ensure that the gestational age was similar to that in the PE group. The clinicopathological data of each patient are shown in Table I. Samples were obtained from the maternal surface of the placental tissue from each patient, and once the blood had been thoroughly washed off, the samples were stored in liquid nitrogen (-196°C) within 15 min of surgery and then stored at -80°C . The Ethics Committee of The First Hospital of China Medical University approved the present study (approval no. AF-SOP-07-1.1-01), and all patients participating in the study signed informed consent forms prior to participation.

Cell lines and culture. The human EVT cell line (HTR-8/SVneo cells) was provided by Dr Charles Graham (College of Life Sciences, Queen's University, Kingston, ON, Canada). The cells were cultured in RPMI-1640 medium (Gibco; Thermo Fisher Scientific, Inc.) supplemented with 10% FBS (HyClone; Cytiva) and maintained at 37°C with 5% CO_2 .

Cell transfection. miR-372-3p inhibitor (5'-GCUCAAUGUCGAGCACUUUUU-3'), inhibitor-negative control (inhibitor-NC; 5'-UUCUCCGAACGUGUCACGUTT-3'), miR-372-3p mimic (5'-AAAGUCGUCGACAUUUGAGCGUCUCAAUGUCGAGCACUUUUU-3') and mimic-NC (5'-ACGUGACAGUUCGGAGAATT-3') (Mass/concentration, 250 μl) were purchased from Guangzhou RiboBio Co., Ltd. Short hairpin (sh)RNA targeting twist family bHLH transcription factor 1 (twist1; sh-twist1), sh-NC, twist1 overexpression plasmid and empty vector (twist1-NC) were purchased from Beijing Syngentech Co., Ltd. Cells were seeded into 6-well plates at a density of 2×10^5 cells/well at 37°C for 48 h and were subsequently transfected with each oligonucleotide or plasmid (250 μl) using Lipofectamine®

3000 (Invitrogen; Thermo Fisher Scientific, Inc.) according to the manufacturer's protocol (temperature and duration of transfection, 37°C).

Reverse transcription-quantitative PCR (RT-qPCR). Total RNA was extracted from tissues and cells using TRIzol® reagent (Invitrogen; Thermo Fisher Scientific, Inc.). The purity and concentration of the RNA was analyzed using a NanoDrop ND-1000 spectrophotometer (Thermo Fisher Scientific, Inc.) at an optical density of 260/280 nm. Total RNA was reverse transcribed into cDNA using random primers from the Transcriptor First Strand cDNA Synthesis kit (Roche Applied Science). RT kit was used according to the manufacturer's protocol. qPCR was subsequently performed on a ViiA 7 Real-Time PCR system (Applied Biosystems; Thermo Fisher Scientific, Inc.). SYBR GREEN mastermix (Takara Bio, Inc.) fluorophore used for the qPCR. The following thermocycling conditions were used for the qPCR: Initial denaturation at 95°C for 10 min; followed by 40 cycles of 95°C for 10 sec, 60°C for 60 sec and 95°C for 15 sec. Primer sequences: MiR-372-3p forward, 5'-TTTCACGACGCTGTAAACTCGCA-3' and reverse, 5'-GTGCAGGGTCCGAGGT-3'; twist1 forward, 5'-TGAATGCATTTAGACACCG-3', and reverse, 5'-AGAGGAAGTCGATGTACCT-3'; GAPDH forward, 5'-GGGAAACTGTGGCGTGAT-3', and reverse, 5'-GAGTGGGTGTCGCTGTTGA-3'; U6 forward, 5'-AACGCTTCACGAATTGCGT-3', and reverse, 5'-CTCGCTTCGGCAGCAC-3'. The relative expression levels were quantified using the $2^{-\Delta\Delta\text{Cq}}$ method (13), using GAPDH or U6 as the controls to normalize the expression levels of mRNAs and miRNAs, respectively.

Transwell assays. HTR-8/SVneo cells were cultured in six-well plates at a density of 1×10^5 cells/well. After transfection, the cells were plated into the upper chambers of Transwell plates (pore size, 8- μm ; Corning, Inc.), which were precoated (37°C ; 2 h) with 50 μl Matrigel or without (BD Biosciences) for the invasion and migration assays, respectively. The lower chambers were filled with RPMI-1640 medium supplemented with 10% FBS. The cells were cultured for 24 or 48 h for the migration or invasion assays, respectively, at 37°C . Following the incubation, the cells remaining in the upper chambers were removed with cotton swabs, and the cells in the lower chambers were fixed with methanol (4%; 25 min) and stained with crystal violet (0.4%; 5 min) at 37°C . Stained cells were visualized (magnification, $\times 200$) using a light microscope. The experiment was independently repeated three times.

Wound healing assay. HTR-8/SVneo cells were cultured in six-well plates at a density of 1×10^5 cells/well. Cells were evenly distributed (70% confluency). An artificial wound was subsequently made in the cell monolayer by scratching the cells with a 200- μl pipette tip and non-adherent cells were removed by three washes with PBS. Serum-free RPMI-1640 medium was added to each well and cells were incubated for 48 h at 37°C with 5% CO_2 . Images of the wound were obtained at 0 and 48 h at the same position. Cell migration rate = (0 h scratch width - scratch width after 48 h) / 0 h scratch width $\times 100\%$. The images were captured using light microscope. The experiment was independently repeated three times.

Table I. Clinical characteristics of patients in the present study.

Variable	Tissue					P-value			
	EOPE, n=18	LOPE, n=13	ENP, n=13	NP, n=15	F-value	P-value	EOPE vs. LOPE tissues	EOPE vs. ENP tissues	LOPE vs. NP tissues
Maternal age, years	29.72±4.47	30.54±3.36	27.38±3.20	31.93±4.23	3.24	<0.05	0.57	0.11	0.35
Gestational age, weeks	31.60±1.55	37.26±0.99	32.01±2.77	38.94±0.57	71.21	<0.05	<0.05	0.48	0.63
Body mass index, kg/m ²	29.76±2.55	31.23±3.57	29.55±3.29	28.47±4.51	1.45	0.24	0.26	0.87	<0.05
Systolic blood pressure, mmHg	172.28±14.70	168.38±11.99	118.77±19.55	113.07±7.63	75.95	<0.05	0.45	<0.05	<0.05
Diastolic blood pressure, mmHg	114.83±13.01	106.15±10.42	78.31±15.61	70.47±8.92	47.27	<0.05	0.06	<0.05	<0.05
24-h proteinuria quantification, g/24	12.73±9.31	7.61±6.36	-	-	17.26	<0.05	<0.05	-	-
Proteinuria level, mg/dl	954.82±765.41	629.74 ±596.06	-	-	13.73	<0.05	0.09	-	-
Urine, ml/24 h	1,605.00±705.88	1,338.46±386.30	1,080.77±149.36	1,260.00±289.83	3.50	<0.05	0.12	<0.05	0.66
PLT, 10 ⁹ /l	163.22±55.72	174.85±60.04	221.77±39.01	219.67±49.62	5.14	<0.05	0.54	<0.05	<0.05
AST, U/l	36.06±24.80	26.85±18.58	20.77±10.43	14.53±4.60	4.66	<0.05	0.15	<0.05	0.06
ALT, U/l	28.72±22.37	21.08±13.91	18.23±10.30	12.40±3.42	3.40	<0.05	0.17	0.06	0.13
Creatinine, mg/dl	0.86±0.31	0.75±0.25	0.58±0.08	0.62±0.08	5.64	<0.05	0.17	<0.05	0.10
Birth weight, g	1,607.78±389.86	2,826.15±392.21	2,413.85±294.29	3,619.33±366.30	85.71	<0.05	<0.05	<0.05	<0.05
Birth length, cm	37.39±3.42	46.38±1.94	40.92±6.34	51.00±1.36	41.67	<0.05	<0.05	<0.05	<0.05
Apgar score, 1 min	8.28±1.07	9.62±0.51	9.31±0.63	10.00±0.00	18.18	<0.05	<0.05	<0.05	0.16

Data are presented as the mean ± SD. ALT, alanine transaminase; PLT, platelet count test; AST, aspartate aminotransferase; ALT, alanine transaminase; PE, preeclampsia; EOPE, early-onset PE; LOPE, late-onset PE; NP, placenta tissues from women who had a full-term delivery; ENP: placenta tissues from women who had a premature delivery; PE, preeclampsia; PLT, platelet count test.

Western blotting. Total protein was extracted from cells using RIPA lysis buffer (Beyotime Institute of Biotechnology). Proteins were quantified using the BCA method. Total protein (10 μ l per lane) was quantified and then separated by 10% SDS-PAGE. The separated proteins were subsequently transferred onto polyvinylidene difluoride membranes (Bio-Rad Laboratories, Inc.) and blocked using 5% (M/V) skimmed milk powder prepared with TBST buffer for 1 h at 4°C (0.1% tween). The membranes were then incubated overnight at 4°C with the following primary antibodies: Anti-E-cadherin (1:1,000; cat. no. 14472S; Cell Signaling Technology, Inc.), anti-vimentin (1:1,000; cat. no. 5741S; Cell Signaling Technology, Inc.), anti-N-cadherin (1:1,500; cat. no. 13116S; Cell Signaling Technology, Inc.), anti-twist1 (1:1,000; cat. no. 69366S; Cell Signaling Technology, Inc.) and anti-GAPDH (1:1,000; cat. no. 5174S). Following the primary antibody incubation, the membranes were washed with TBST and incubated with HRP-conjugated secondary antibodies goat anti-rabbit (1:1,000; cat. no. GTX213110-01; GeneTex) and anti-mouse antibodies (1:1,000; cat. GTX213111-01; GeneTex) for 2 h at 4°C. Protein bands were visualized using ECL reagent (Beyotime Institute of Biotechnology). GAPDH was used as the internal loading control.

Dual luciferase reporter assay. A dual luciferase reporter assay (Luciferase detection kit; cat. no. E1910; Promega Corporation) was performed to determine the interaction between miR-372-3p and twist1. The entire sequence of twist1 containing the wild-type (WT) 3'-untranslated region (UTR) with the predicted target site of miR-372-3p (LUC-twist1-WT) or a mutant-type (Mut) 3'-UTR target site (LUC-twist1-Mut) was subcloned into the pmirGLO vector (Syngentech Co., Ltd.). Then, 293T cells (National Collection of Authenticated Cell Cultures) were seeded into 24-well plates at a density of 5×10^5 cells/well and co-transfected with either LUC-twist1-Mut or -WT vectors and either miR-372-3p mimic or mimic-NC using Lipofectamine® 2000 (Invitrogen; Thermo Fisher Scientific, Inc.). Following 48 h of transfection, the relative firefly luciferase activity was measured and normalized to *Renilla* luciferase activity.

Statistical analysis. Statistical analysis was performed using SPSS 22.0 software (IBM Corp.), and data are presented as the mean \pm SD. Each experiment was repeated three times independently. Statistical differences between three or more groups were determined using a one-way ANOVA followed by a Bonferroni's post hoc test. Statistical differences between two groups were determined using an unpaired Student's t-test. Pearson's correlation analysis was performed to analyze the correlation between two groups. Bioinformatics analysis used the following databases: RNA22 v2 (<https://cm.jefferson.edu>); RNAhybrid (<https://bibiserv.cebitec.uni-bielefeld.de/rnahybrid>). $P < 0.05$ was considered to indicate a statistically significant difference.

Results

miR-372-3p expression levels are upregulated in PE tissues. RT-qPCR was performed to analyze the expression levels of miR-372-3p in PE tissues. The expression levels of miR-372-3p

were upregulated in PE tissues compared with placenta tissues from women who had a full-term delivery (NP tissues) (Fig. 1A). According to the gestational age, PE tissues were divided into EOPE (≤ 34 weeks) and LOPE (> 34 weeks) tissues, which have differential pathogenesis. As shown in Table I, there were statistically significant differences in clinical characteristics such as systolic blood pressure, systolic blood pressure, 24-h urine protein, ALT, AST and creatinine between the preeclampsia group (EOPE, LOPE) and the control group (ENP, NP). EOPE is considered to originate from complications in the placenta, such as trophoblast dysfunction and insufficient spiral artery remodeling (14,15). By contrast, LOPE is considered to be of maternal origin and can arise from metabolic disorders and endothelial cell dysfunction (16,17). RT-qPCR results revealed that the expression levels of miR-372-3p were upregulated in EOPE tissues compared with the pre-term delivery (ENP) and NP groups (Fig. 1B). In addition, the expression levels of miR-372-3p were upregulated in the LOPE group compared with the NP group, which suggested that miR-372-3p may be closely associated with PE. Moreover, miR-372-3p expression levels were upregulated in the EOPE group compared with the LOPE group, which suggested that miR-372-3p may be associated with trophoblast function. Overall, the results suggested that miR-372-3p may serve a regulatory role over trophoblast behaviors.

miR-372-3p regulates trophoblast cell migration, invasion and EMT. To investigate the function of miR-372-3p in trophoblast cells, miR-372-3p was successfully overexpressed or knocked down by transfection of a miR-372-3p mimic or inhibitor into HTR-8/SVneo cells, respectively (Fig. 1C). The results of the Transwell and Matrigel assays revealed that the number of migratory and invasive cells, respectively, in the miR-372-3p mimic group was significantly decreased compared with the mimic-NC group, which suggested that miR-372-3p may suppress HTR-8/SVneo cell migration and invasion (Fig. 1D). The opposite results were observed following transfection with the miR-372-3p inhibitor (Fig. 1E). Western blotting was used to analyze the expression levels of several EMT-related proteins to determine if miR-372-3p could modulate EMT in trophoblast cells. The results demonstrated that the expression levels of E-cadherin were upregulated, whereas the expression levels of N-cadherin and vimentin were downregulated following the overexpression of miR-372-3p. The trends in the expression levels of these proteins were the opposite in miR-372-3p-knockdown cells (Fig. 1F). These results suggested that miR-372-3p may suppress trophoblast cell migration, invasion and EMT.

miR-372-3p targets twist1. According to the competing endogenous RNA (ceRNA) theory, circular RNA can compete with mRNA to bind miRNA, thereby affecting the expression of mRNA (18-20). The present study investigated the underlying regulatory mechanism of miR-372-3p on trophoblast cell behavior. Bioinformatics analysis predicted that the 3'-UTR of twist1 was targeted by miR-372-3p (Fig. 2A). A dual luciferase reporter assay was used to validate the binding relationship between miR-372-3p and twist1. The relative luciferase activity of the Twist1-WT vector was significantly decreased when co-transfected with the miR-372-3p mimic compared

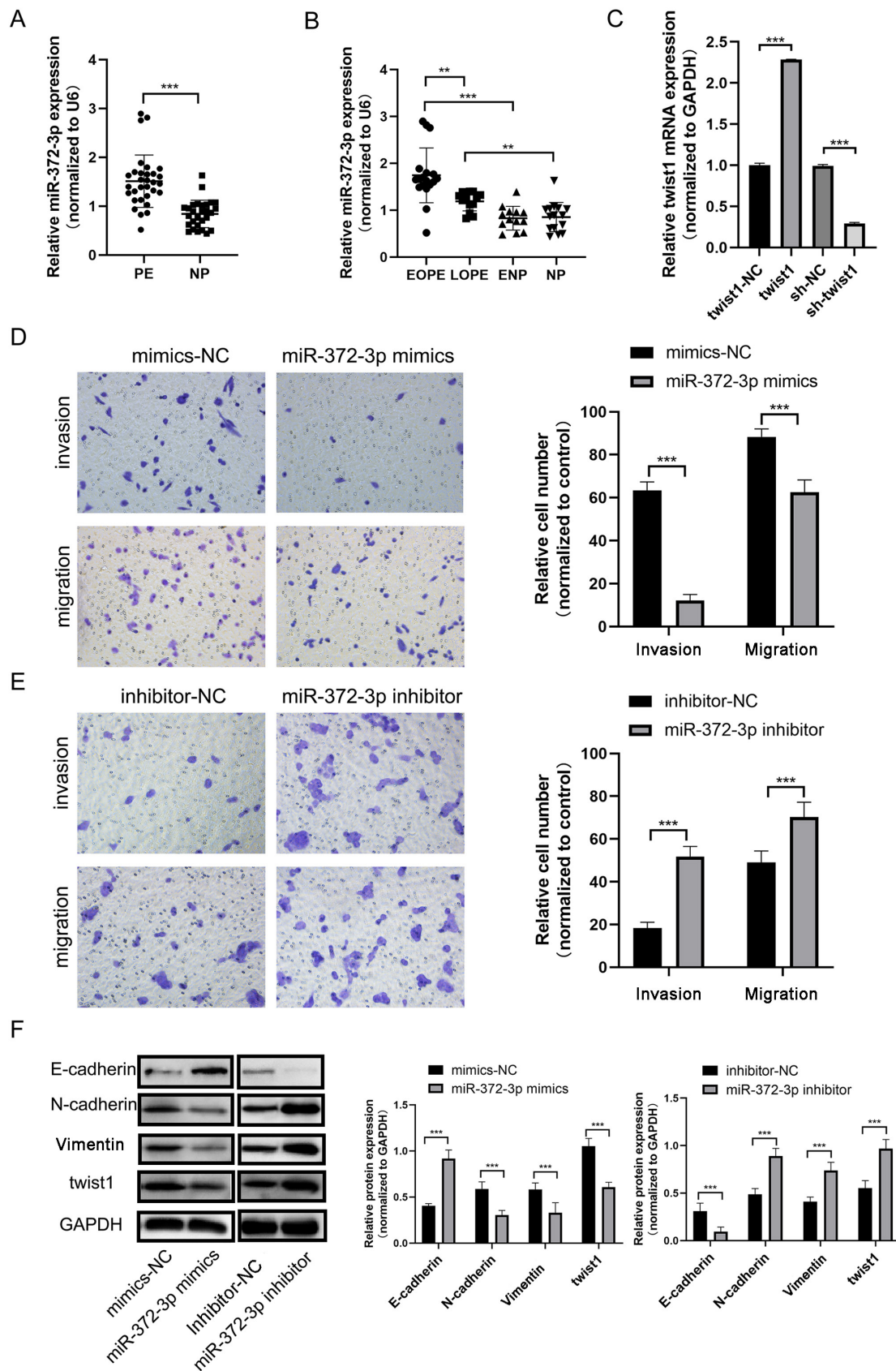


Figure 1. miR-372-3p expression levels in PE. (A) RT-qPCR was performed to analyze miR-372-3p expression levels in PE and NP tissues. (B) RT-qPCR was performed to determine miR-372-3p expression among EOPE, LOPE, ENP and NP. (C) RT-qPCR was performed to verify the transfection efficiency of the miR-372-3p mimic and inhibitor into HTR-8/Svneo cells. Transwell assays were performed to evaluate HTR-8/Svneo cell migration and invasion following transfection with the (D) miR-372-3p mimic or (E) miR-372-3p inhibitor (magnification, x200). (F) Western blotting was used to analyze the expression levels of epithelial-mesenchymal transition-related proteins. Data are presented as the mean \pm SD. ** $P < 0.01$ and *** $P < 0.001$. miR, microRNA; RT-qPCR, reverse transcription-quantitative PCR; PE, preeclampsia; EOPE, early-onset PE; LOPE, late-onset PE; NP tissues, placenta tissues from women who had a full-term delivery; PE tissues, placenta tissues from patients with PE; NC, negative control; twist1, twist family bHLH transcription factor 1; ENP, placenta tissues from women who had a premature delivery.

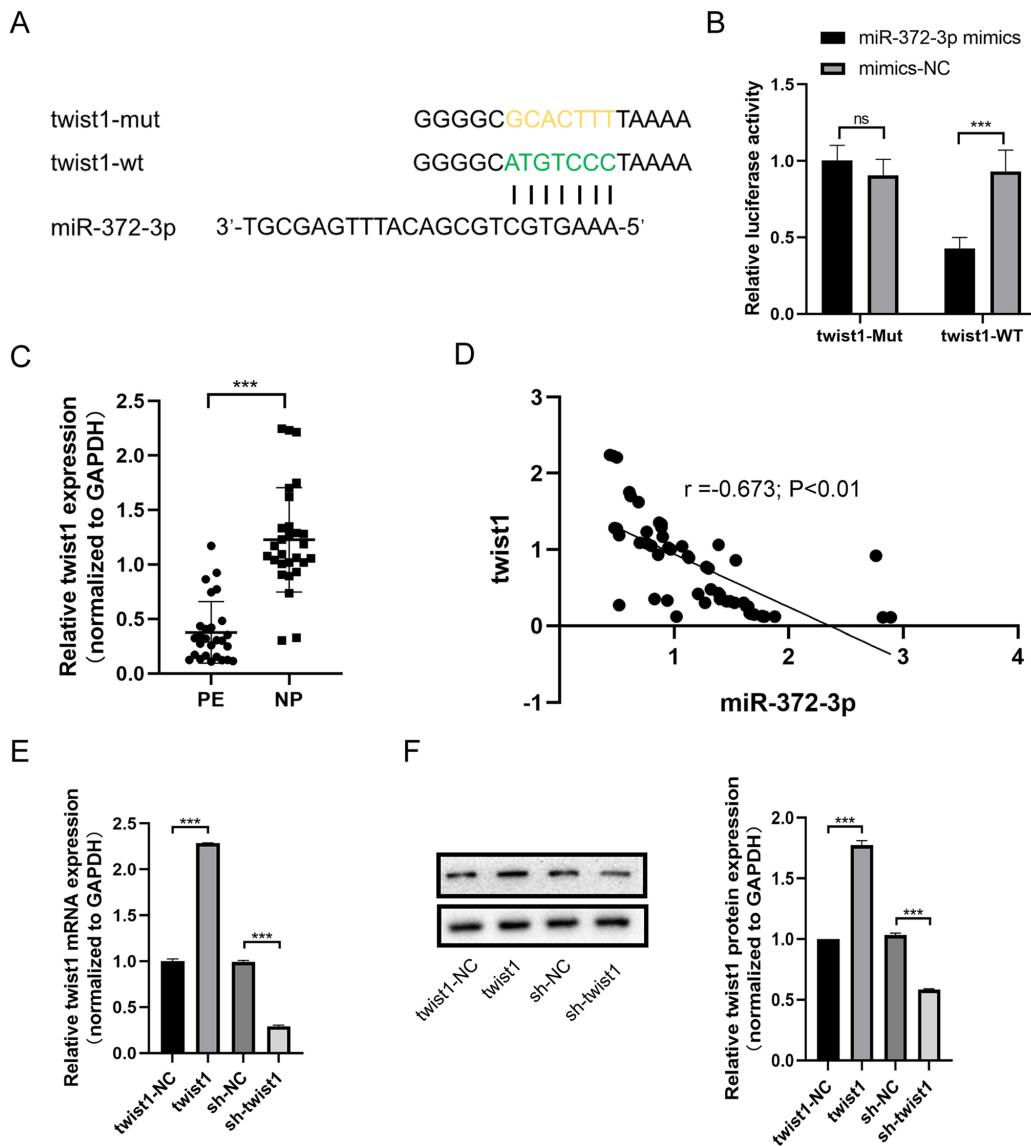


Figure 2. miR-372-3p targets Twist1. (A) Schematic diagram of WT and Mut 3'-UTR sequences of miR-372-3p targeting twist1. (B) Dual luciferase reporter assays were used to evaluate the relative luciferase activity of LUC-twist1-WT or -Mut vectors co-transfected with miR-372-3p mimic or mimic-NC. (C) RT-qPCR was used to analyze the expression levels of twist1 in PE and NP tissues. (D) Correlation analysis of miR-372-3p and twist1 expression. (E) RT-qPCR and (F) western blotting were performed to verify the transfection efficiency of twist1 overexpression vector and sh-twist1. Data are presented as the mean \pm SD. *** $P < 0.001$. NS, no significance; twist1, twist family bHLH transcription factor 1; miR, microRNA; WT, wild-type; Mut, mutant-type; NC, negative control; PE tissues, placenta tissues from patients with preeclampsia; NP tissues, placenta tissues from women who had a full-term delivery; sh-, short hairpin RNA.

with the mimic-NC (Fig. 2B). However, the relative luciferase activity of the Twist1-Mut vector was unchanged between cells co-transfected with the miR-372-3p mimic or mimic-NC. (Fig. 2B). RT-qPCR was performed to analyze the expression levels of twist1 in PE and NP tissues, and the results revealed that the expression levels of twist1 were lower in PE tissues compared with those in NP tissues (Fig. 2C). Moreover, the expression levels of miR-372-3p and twist1 were found to be negatively correlated in the tissues including PE and NP ($r = -0.673$; $P < 0.01$; Fig. 2D).

miR-372-3p suppresses trophoblast cell migration, invasion and EMT by targeting twist1. Rescue experiments were performed by co-transfecting cells with miR-372-3p mimic and twist1 overexpression vector to determine their effects on

trophoblast cell behaviors. As shown in Fig. 2E and F, twist1 was successfully overexpressed or knocked down at both the mRNA and protein levels (Fig. 2E and F). The wound healing assay results showed that the cell migration rate was decreased in the miR-372-3p mimic group compared with the mimic-NC group, whereas migration was increased in the miR-372-3p mimic + twist1 group compared with the miR-372-3p mimic group (Fig. 3A). The opposite trends were observed in cells co-transfected with the miR-372-3p inhibitor and sh-twist1 (Fig. 3B). The Transwell and Matrigel assay results revealed that the number of migratory and invasive cells, respectively, in the miR-372-3p mimic group was decreased compared with the mimic-NC group, whereas cell invasion and migration were increased in the miR-372-3p mimic + twist1 group compared with the miR-372-3p mimic group (Fig. 3C); the

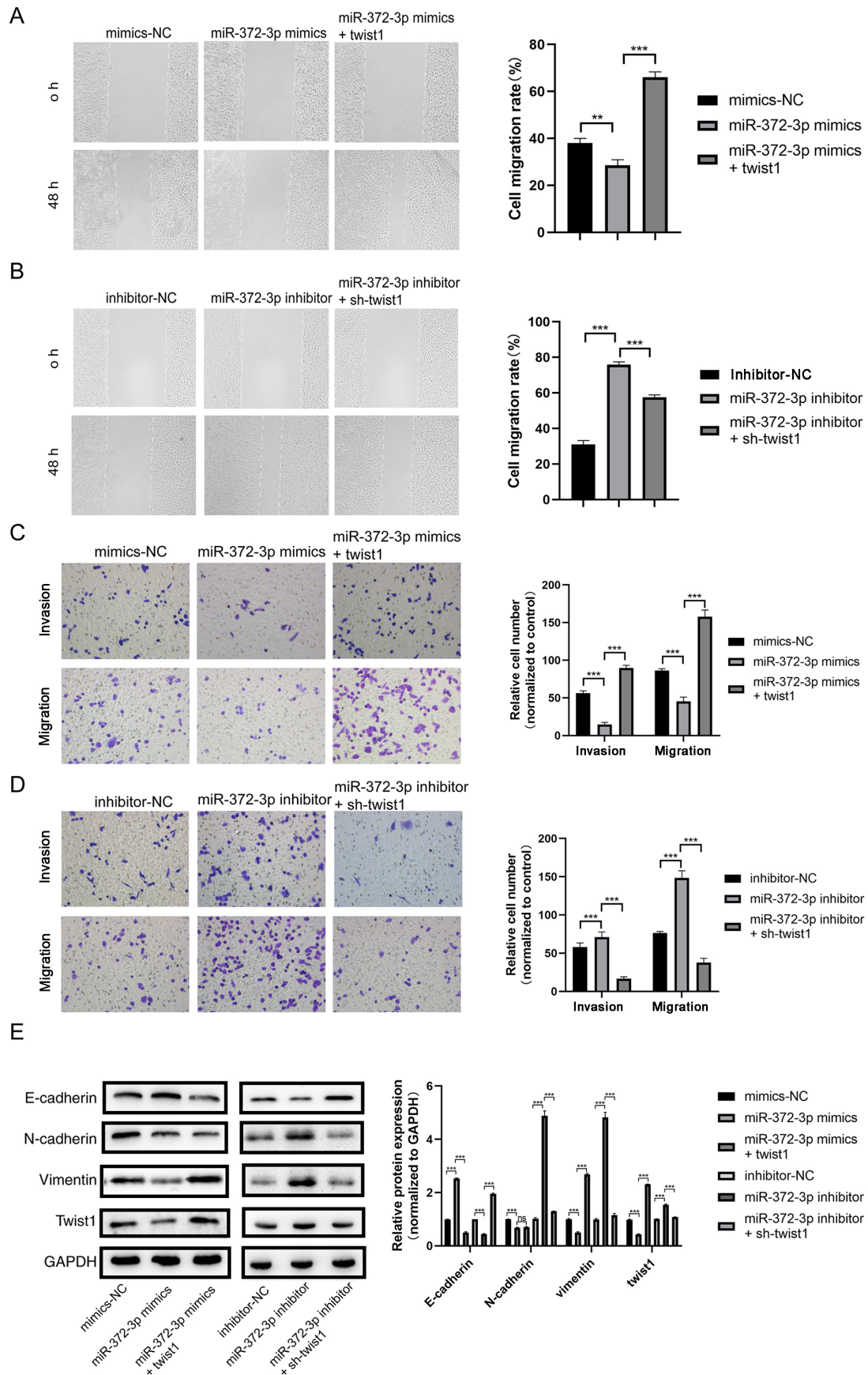


Figure 3. miR-372-3p modulates trophoblast cell migration, invasion and epithelial-mesenchymal transition by regulating twist1. Wound healing assays were performed to determine cell migration following the transfection with (A) miR-372-3p mimic with or without twist1 overexpression vector and (B) miR-372-3p inhibitor with or without sh-twist1 (magnification, x100). Transwell and Matrigel assays were used to detect cell migration and invasion, respectively, following the transfection with (C) miR-372-3p mimic with or without twist1 overexpression vector and (D) miR-372-3p inhibitor with or without sh-twist1 (magnification, x200). (E) Western blotting was used to analyze the expression levels of epithelial-mesenchymal transition-related proteins. Data are presented as the mean \pm SD. **P<0.01, ***P<0.001.

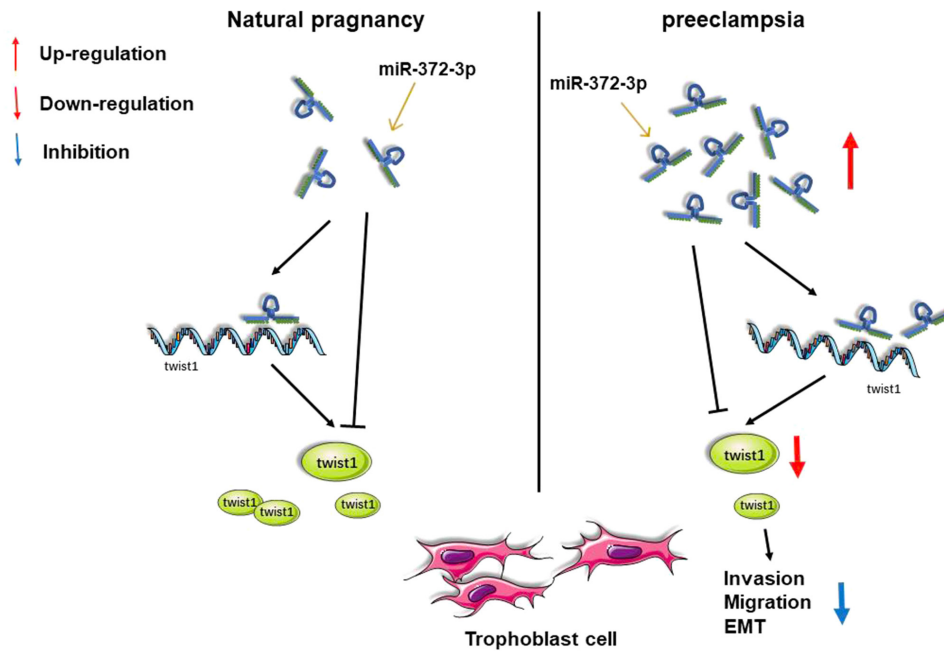


Figure 4. Schematic diagram of miR-372-3p-induced modulation of trophoblast cell migration, invasion and EMT through the regulation of twist1. miR, microRNA; EMT, epithelial-mesenchymal transition; twist1, twist family bHLH transcription factor.

opposite trends were observed in cells co-transfected with the miR-372-3p inhibitor and sh-twist1 (Fig. 3D). These results suggested that twist1 may reverse the effects of miR-372-3p on trophoblast cell migration and invasion.

The results of the western blotting analysis demonstrated that the expression levels of E-cadherin were upregulated following the transfection with the miR-372-3p mimic compared with those in the mimic-NC group, whereas these effects were reversed following the co-transfection with the miR-372-3p mimic and twist1 (Fig. 3E). The expression levels of N-cadherin, vimentin and twist1 in the miR-372-3p mimic group was lower than the co-transfection group, which indicated that twist1 reverse miR-372-3p-modulated EMT in trophoblasts (Fig. 3E). The expression of E-cadherin in the miR-372-3p inhibitor group was significantly lower compared with that of the miR-372-3p inhibitor + sh-twist1 group, while N-cadherin, vimentin and twist1 expression levels in the miR-372-3p inhibitor group were higher compared the co-transfection group (Fig. 3E).

Discussion

PE progression is a long and complicated process that can be divided into six stages: i) The mother first develops immune intolerance to the paternal genes of the embryo between the fertilization and implantation stages of the embryo; ii) abnormal placenta formation occurs and trophoblast invasion into the uterine spiral artery is decreased during the 8-18th weeks of pregnancy, which is an important period of placental development; iii) the stress response is activated; iv) various placental-derived injury factors are released into the maternal blood circulation during the second half of the pregnancy; v) clinical symptoms, such as hypertension, which enable the clinical diagnosis of PE, appear; and vi) an acute illness is exacerbated in half

of the patients, atherosclerosis in the spiral artery rapidly develops, placental perfusion is further reduced and spiral artery thrombosis and even placental infarction are induced. Owing to the early occurrence and long duration of the second stage of this process, the trophoblasts invading the spiral artery from the 8th week participate in the formation of the placenta. This stage is considered to be the key step for triggering the development of PE and can subsequently activate signaling molecules to create a cascading amplification effect, causing continuous damage at the maternal-fetal interface. Therefore, this stage is the most crucial period for studying the pathophysiological changes of trophoblasts and for identifying biomarkers for the early prediction and diagnosis of PE.

During the process of placental implantation in early pregnancy, extraembryonic trophoblast cells differentiate into syncytiotrophoblast cells and extravillous cytotrophoblast cells (3). Syncytiotrophoblasts are trophoblasts with a secretory phenotype, which are distributed on the surface of the placenta and secrete cytokines to maintain the normal development of the placenta. The proximal extravillous cytotrophoblasts near the fetal side acquire a proliferative phenotype, whereas the distal extravillous cytotrophoblasts acquire a migratory and invasive phenotype (3,21). In more detail, the morphology of these trophoblasts changes from a rounded epithelial cell to a more elongated, mesenchymal phenotype, with enhanced migratory and invasive abilities that enables the placenta to firmly anchor onto the decidua (4). This cellular morphology transformation is also called trophoblast EMT (4). Several EMT-related proteins, such as E-cadherin, N-cadherin, vimentin and twist1, were discovered to be differentially expressed during the transition (4,21).

miRNAs are short non-coding RNAs that are highly conserved throughout evolution (22,23). Owing to their long half-life and high stability in extracellular fluid, such as serum,

plasma and urine, miRNAs are suggested to be more suitable diagnostic biomarkers than mRNAs (24,25). Previous studies have reported that miRNAs served roles in numerous mechanisms in various diseases, such as prostate cancer, ovarian cancer and Alzheimer's (26-28). In PE, several miRNAs were found to be differentially expressed in the circulation, decidua-derived mesenchymal stem cells, amniotic fluid and placenta (29-31). Thus, whether miRNAs can regulate PE progression should be studied in further depth in the future.

It has been proposed that some protein-coding transcripts can act as endogenous miRNA sponges, which are also known as ceRNAs (20). ceRNAs communicate with and co-regulate each other by competing for the binding to shared miRNAs, thereby sequestering miRNA availability (20). Co-transfection of miR-372-3p (mimics/inhibitors) and *twist1* (mimics/inhibitors) demonstrated that *twist1* could partially reverse the effects of miR-372-3p (mimics/inhibitors) on trophoblast cells, which suggested that miR-372-3p may suppress trophoblast migration, invasion and EMT (E-cadherin, N-cadherin, vimentin and *twist1*) by targeting *twist1*. Previous studies have reported that miR-372-3p serves important roles in numerous types of disease, for example colorectal cancer, lung squamous cell carcinoma, osteosarcoma, hepatocellular carcinoma (8,32-36).

In conclusion, to the best of our knowledge, the present study was the first to identify the role of miR-372-3p in PE. miR-372-3p was revealed to suppress trophoblast cell invasion, migration and EMT via inhibiting *twist1* (Fig. 4). In future studies, a larger sample size will be used, and the expression levels of miR-372-3p in the peripheral blood and placenta from women of different gestational weeks will be investigated to verify the role of miR-372-3p in PE.

Acknowledgements

Not applicable.

Funding

The present study was supported by The National Natural Science Foundation (grant no. 81871173).

Availability of data and materials

The datasets used and/or analyzed during the current study are available from the corresponding author on reasonable request.

Authors' contributions

ZL conceived and designed the experiments, performed the experiments, analyzed the data and wrote the manuscript; JW and HC collected the clinical data and sample tissues, and participated in drafting the manuscript or revising it critically for important content; DL collected the clinical data and sample tissues and participated in the design of experimental ideas. TM designed the study and supervised the progression of the project as the corresponding author. All authors have read and approved the final manuscript. ZL and TM confirm the authenticity of all the raw data.

Ethics approval and consent to participate

The Ethics Committee of The First Hospital of China Medical University approved the present study (approval no. AF-SOP-07-1.1-01), and all patients participating in the study signed informed consent prior to participation.

Patient consent for publication

Not applicable.

Competing interests

The authors declare that they have no competing interests.

References

1. No authors listed: Gestational hypertension and preeclampsia: ACOG practice bulletin, number 222. *Obstet Gynecol* 135: e237-e260, 2020.
2. Shen XY, Zheng LL, Huang J, Kong HF, Chang YJ, Wang F and Xin H: CircTRNC18 inhibits trophoblast cell migration and epithelial-mesenchymal transition by regulating miR-762/Grhl2 pathway in pre-eclampsia. *RNA Biol* 16: 1565-1573, 2019.
3. E Davies J, Pollheimer J, Yong HE, Kokkinos MI, Kalionis B, Knofler M and Murthi P: Epithelial-mesenchymal transition during extravillous trophoblast differentiation. *Cell Adh Migr* 10: 310-321, 2016.
4. DaSilva-Arnold SC, Zamudio S, Al-Khan A, Alvarez-Perez J, Mannion C, Koenig C, Luke D, Perez AM, Petroff M, Alvarez M, *et al*: Human trophoblast epithelial-mesenchymal transition in abnormally invasive placenta. *Biol Reprod* 99: 409-421, 2018.
5. Moldovan L, Batte KE, Trgovcich J, Wisler J, Marsh CB and Piper M: Methodological challenges in utilizing miRNAs as circulating biomarkers. *J Cell Mol Med* 18: 371-390, 2014.
6. Cai Z, Li J, Zhuang Q, Zhang X, Yuan A, Shen L, Kang K, Qu B, Tang Y, Pu J, *et al*: MiR-125a-5p ameliorates monocrotaline-induced pulmonary arterial hypertension by targeting the TGF- β 1 and IL-6/STAT3 signaling pathways. *Exp Mol Med* 50: 1-11, 2018.
7. Shi J, Zhang Y, Jin N, Li Y, Wu S and Xu L: MicroRNA-221-3p plays an oncogenic role in gastric carcinoma by inhibiting PTEN expression. *Oncol Res* 25: 523-536, 2017.
8. Peng H, Pan X, Su Q, Zhu LS and Ma GD: MiR-372-3p promotes tumor progression by targeting LATS2 in colorectal cancer. *Eur Rev Med Pharmacol Sci* 23: 8332-8344, 2019.
9. Chen DB and Wang W: Human placental microRNAs and preeclampsia. *Biol Reprod* 88: 130, 2013.
10. Lv Y, Lu X, Li C, Fan Y, Ji X, Long W, Meng L, Wu L, Wang L, Lv M and Ding H: miR-145-5p promotes trophoblast cell growth and invasion by targeting FLT1. *Life Sci* 239: 117008, 2019.
11. Brkić J, Dunk C, O'Brien J, Fu G, Nadeem L, Wang YL, Rosman D, Salem M, Shynlova O, Yougbaré I, *et al*: MicroRNA-218-5p promotes endovascular trophoblast differentiation and spiral artery remodeling. *Mol Ther* 26: 2189-2205, 2018.
12. Yang Y, Li H, Ma Y, Zhu X, Zhang S and Li J: MiR-221-3p is down-regulated in preeclampsia and affects trophoblast growth, invasion and migration partly via targeting thrombospondin 2. *Biomed Pharmacother* 109: 127-134, 2019.
13. Livak KJ and Schmittgen TD: Analysis of relative gene expression data using real-time quantitative PCR and the 2(-Delta Delta C(T)) method. *Methods* 25: 402-408, 2001.
14. Tayyar AT, Karakus R, Eraslan Sahin M, Topbas NF, Sahin E, Karakus S, Yalcin ET and Tayyar A: Wnt signaling pathway in early- and late-onset preeclampsia: Evaluation with Dickkopf-1 and R-Spondin-3 glycoproteins. *Arch Gynecol Obstet* 299: 1551-1556, 2019.
15. von Dadelszen P, Magee LA and Roberts JM: Subclassification of preeclampsia. *Hypertens Pregnancy* 22: 143-148, 2003.
16. Herzog EM, Eggink AJ, Reijnierse A, Kerkhof MA, de Krijger RR, Roks AJ, Reiss IK, Nigg AL, Eilers PH, Steegers EA, *et al*: Impact of early- and late-onset preeclampsia on features of placental and newborn vascular health. *Placenta* 49: 72-79, 2017.

17. Cim N, Kurdoglu M, Ege S, Yoruk I, Yaman G and Yildizhan R: An analysis on the roles of angiogenesis-related factors including serum vitamin D, soluble endoglin (sEng), soluble fms-like tyrosine kinase 1 (sFlt1), and vascular endothelial growth factor (VEGF) in the diagnosis and severity of late-onset preeclampsia. *J Matern Fetal Neonatal Med* 30: 1602-1607, 2017.
18. Karreth FA and Pandolfi PP: ceRNA cross-talk in cancer: When ce-bling rivalries go awry. *Cancer Discov* 3: 1113-1121, 2013.
19. Yang R, Xing L, Zheng X, Sun Y, Wang X and Chen J: The circRNA circAGFG1 acts as a sponge of miR-195-5p to promote triple-negative breast cancer progression through regulating CCNE1 expression. *Mol Cancer* 18: 4, 2019.
20. Tay Y, Rinn J and Pandolfi PP: The multilayered complexity of ceRNA crosstalk and competition. *Nature* 505: 344-352, 2014.
21. Kalluri R and Weinberg RA: The basics of epithelial-mesenchymal transition. *J Clin Invest* 119: 1420-1428, 2009.
22. Beermann J, Piccoli MT, Viereck J and Thum T: Non-coding RNAs in development and disease: Background, mechanisms, and therapeutic approaches. *Physiol Rev* 96: 1297-1325, 2016.
23. Lee CT, Risom T and Strauss WM: Evolutionary conservation of microRNA regulatory circuits: An examination of microRNA gene complexity and conserved microRNA-target interactions through metazoan phylogeny. *DNA Cell Biol* 26: 209-218, 2007.
24. Gantier MP, McCoy CE, Rusinova I, Saulep D, Wang D, Xu D, Irving AT, Behlke MA, Hertzog PJ, Mackay F and Williams BR: Analysis of microRNA turnover in mammalian cells following Dicer1 ablation. *Nucleic Acids Res* 39: 5692-5703, 2011.
25. Sayed AS, Xia K, Salma U, Yang T and Peng J: Diagnosis, prognosis and therapeutic role of circulating miRNAs in cardiovascular diseases. *Heart Lung Circ* 23: 503-510, 2014.
26. Sur S, Steele R, Shi X and Ray RB: miRNA-29b inhibits prostate tumor growth and induces apoptosis by increasing bim expression. *Cells* 8, 1455, 2019.
27. Ghafouri-Fard S, Shoorei H and Taheri M: miRNA profile in ovarian cancer. *Exp Mol Pathol* 113: 104381, 2020.
28. Hansen TB, Jensen TI, Clausen BH, Bramsen JB, Finsen B, Damgaard CK and Kjems J: Natural RNA circles function as efficient microRNA sponges. *Nature* 495: 384-388, 2013.
29. Hromadnikova I, Kotlabova K, Ivankova K, Vedmetuskaya Y and Krofta L: Profiling of cardiovascular and cerebrovascular disease associated microRNA expression in umbilical cord blood in gestational hypertension, preeclampsia and fetal growth restriction. *Int J Cardiol* 249: 402-409, 2017.
30. Zhao G, Zhou X, Chen S, Miao H, Fan H, Wang Z, Hu Y and Hou Y: Differential expression of microRNAs in decidua-derived mesenchymal stem cells from patients with pre-eclampsia. *J Biomed Sci* 21: 81, 2014.
31. Zhou C, Zou QY, Li H, Wang RF, Liu AX, Magness RR and Zheng J: Preeclampsia downregulates MicroRNAs in fetal endothelial cells: Roles of miR-29a/c-3p in endothelial function. *J Clin Endocrinol Metab* 102: 3470-3479, 2017.
32. Wang Q, Liu S, Zhao X, Wang Y, Tian D and Jiang W: MiR-372-3p promotes cell growth and metastasis by targeting FGF9 in lung squamous cell carcinoma. *Cancer Med* 6: 1323-1330, 2017.
33. Li Y, Liu JJ, Zhou JH, Chen R and Cen CQ: LncRNA HULC induces the progression of osteosarcoma by regulating the miR-372-3p/HMGB1 signalling axis. *Mol Med* 26: 26, 2020.
34. Fan J, Zhang J, Huang S and Li P: lncRNA OSER1-AS1 acts as a ceRNA to promote tumorigenesis in hepatocellular carcinoma by regulating miR-372-3p/Rab23 axis. *Biochem Biophys Res Commun* 521: 196-203, 2020.
35. Soliman MH, Ragheb MA, Elzayat EM, Mohamed MS, El-Ekiaby N, Abdelaziz AI and Abdel-Wahab AA: MicroRNA-372-3p predicts response of TACE patients treated with doxorubicin and enhances chemosensitivity in hepatocellular carcinoma. *Anticancer Agents Med Chem* 21: 246-253, 2021.
36. Fan X, Huang X, Li Z and Ma X: MicroRNA-372-3p promotes the epithelial-mesenchymal transition in breast carcinoma by activating the Wnt pathway. *J BUON* 23: 1309-1315, 2018.



This work is licensed under a Creative Commons Attribution-NonCommercial-NoDerivatives 4.0 International (CC BY-NC-ND 4.0) License.